Spectrum of Engineering Sciences
ISSN (e) 3007-3138 (p) 3007-312X Volume 4, Issue 3, 2026

MULTI-OBJECTIVE OPTIMIZATION MODEL OF BATTERY SWAPPING STATIONS TO MINIMIZE COST AND BATTERY DEGRADATION

[1]Sher Muhammad Ghoto, [2]Muhammad Kashif Abbasi, [3]Azhar Hussain Shah, [*4]Qadir Bux, [5]Muhamamd Ramzan Luhur

[1,3,4,5]Mechanical Department Quaid-E-Awam University of Engineering Science and Technology Nawabshah, Sindh, Pakistan.

[2]Industrial and Manufacturing Department Quaid-E-Awam University of Engineering Science and Technology Nawabshah, Sindh, Pakistan

*[*4]tunioqadir15@gmail.com*

Keywords
Battery swapping station; multi-objective optimization; Model predictive control; Linearised throughput penalty; V2G regulation; Electric vehicles; CVXPY

Article History
Received on 14 Feb, 2026
Accepted on 12 March, 2026
Published on 15 March, 2026

Corresponding Author:
Qadir Bux

Abstract

Battery Swapping Stations (BSS) offer rapid energy exchange for electric vehicles while functioning as flexible grid assets. This study develops a multi-objective optimization framework utilizing Model Predictive Control (MPC) with convex programming (CVXPY) to balance electricity procurement costs against battery health. We employ a Linearised Throughput Penalty, calibrated from the Wöhler curve at 80% Depth of Discharge (DOD), to serve as a convex proxy for electrochemical degradation. The system is controlled via a 24-hour receding horizon simulated over a 168-hour (one week) operational period to capture diurnal load variances. Cost sensitivity analysis reveals that a conservative degradation penalty (ψ= $0.05/kWh) creates a robust trade- off, achieving a net weekly revenue of $160.08 while limiting Equivalent Full Cycles (EFC) to Preserving levels. Furthermore, V2G regulatory analysis quantifies the impact of export restrictions: prohibiting grid back-feeding generates an opportunity cost of ~$295/week due to curtailed renewable generation. The CVXPY solver demonstrates varying performance based on horizon length, achieving 45 ms computation time for the 24-hour control loop, validating suitability for real-time deployment.

1 Introduction

1.1 Background

The global transition toward sustainable transportation has accelerated electric vehicle (EV) adoption, with global EV sales reaching 14 million units in 2023, representing 18% of total vehicle sales (IEA, 2024). This rapid electrification creates both opportunities and challenges for power system operators regarding charging infrastructure and grid integration (Yang et al., 2021).

Traditional plug-in charging stations require 30 minutes to several hours for full battery replenishment, creating bottlenecks during peak demand periods (Zhang et al., 2017). Battery swapping stations (BSS) present a compelling alternative, enabling complete battery exchanges within 3-5 minutes, comparable to conventional refuelling times (Wang & Wang, 2023). This rapid service model has gained significant traction in markets such as China, where companies like NIO have deployed over 2,000 swapping stations (NIO, 2024).

Beyond rapid service delivery, BSS offer unique advantages as flexible grid assets through vehicle-to-grid (V2G) capability (Kempton & Tomić, 2005). This dual functionality enables BSS operators to participate in electricity markets through time-of-use arbitrage and grid services (Gu et al., 2020). However, regulatory constraints in many jurisdictions limit grid back-feeding without special interconnection agreements (Sovacool et al., 2018), creating operational challenges that must be addressed in optimization frameworks.

The economic viability of BSS depends critically on balancing multiple competing objectives: minimizing electricity procurement costs, preserving battery asset value by limiting degradation- inducing cycling, and maintaining compliance with grid interconnection requirements (Chen et al., 2021). This multi-objective optimization problem becomes particularly complex when considering the non-linear relationship between battery cycling patterns and capacity fade (Xu et al., 2018), the stochastic nature of EV arrival patterns (Li et al., 2020), and time-varying electricity prices in deregulated markets (Wu et al., 2018).

1.2 Problem Statement

BSS operators face a multi-objective challenge balancing:

1. Cost Minimization: Exploiting time-of-use pricing through charge/discharge arbitrage
2. Degradation Minimization: Reducing cycling to preserve battery asset value
3. Regulatory Compliance: Operating within V2G export constraints

1.3 Literature Review

1.3.1 Battery Swapping Station Optimization

The optimization of BSS operations has been extensively studied from multiple perspectives. Chen et al. (2021) developed a comprehensive planning framework for optimal BSS location and sizing, considering user behaviour and travel patterns. Gao et al. (2022) analysed business models and pricing strategies for battery swapping as a service, highlighting the importance of operational efficiency. Sun et al. (2018) proposed optimal scheduling algorithms for EV battery swapping, focusing on minimizing waiting times and maximizing throughput.

Recent work has increasingly recognized the grid services potential of BSS. Gu et al. (2020) investigated optimal operation of BSS with V2G capability, demonstrating revenue opportunities through grid services. Panduranga & Verma (2021) explored optimization of BSS within smart grid contexts, emphasizing the need for coordinated control strategies. Cui et al. (2024) examined peer-to-peer energy trading among multiple BSS, revealing additional value streams through cooperative operation.

1.3.2 Model Predictive Control for Energy Systems

Model Predictive Control (MPC) has emerged as a dominant framework for energy system optimization due to its ability to handle constraints and incorporate forecasts (Parisio et al., 2014). Zhang et al. (2020) specifically applied MPC to BSS profit maximization, achieving significant improvements overrule-based controllers. However, these studies typically employed short prediction horizons (4-6 hours), which may be insufficient for batteries with extended duration capabilities.

1.3.3 Battery Degradation Modelling

Battery degradation modelling has evolved from simple cycle-counting methods to sophisticated electrochemical models (Vetter et al., 2005). Ecker et al. (2014) and Schmalstieg et al. (2014) developed comprehensive aging models that account for both calendar and cycle aging effects, demonstrating the importance of temperature, state-of-charge, and depth-of-discharge in determining battery lifetime. Xu et al. (2018) demonstrated that capacity fade follows a Wöhler curve relationship:

$$N(DOD) = a \times DOD^{-b}$$

where N is cycle life, DOD is depth-of-discharge, a ~ 14,000, and b ~ 1.5 for Lithium Iron Phosphate (LFP) chemistry. This power-law relationship is non-linear and cannot be directly optimized in standard convex solvers without integer variables or significant relaxation (Xu et al., 2018). Marongiu et al. (2016) investigated the influence of V2G strategies on battery aging, finding that frequent shallow cycling can accelerate degradation compared to deeper, less frequent cycles. Uddin et al. (2018) identified degradation costs as a critical barrier to widespread V2G adoption.

1.3.4 Optimization Approaches for Battery Degradation

Several approaches have been proposed to incorporate battery degradation into optimization frameworks. Wang et al. (2022) employed two-stage stochastic programming for BSS operation, using simplified degradation models to maintain computational tractability. Sarker et al. (2016) developed optimization models under-price uncertainty, but simplified degradation to linear throughput penalties. Liu et al. (2023) applied deep reinforcement learning for real-time BSS scheduling, learning degradation patterns implicitly through reward functions.

However, most existing studies either oversimplify degradation (using linear models that ignore DOD dependence) or employ computationally prohibitive non-linear models that preclude real- time implementation. This gap motivates the development of a convex approximation that captures the essential degradation behaviour while maintaining computational efficiency.

1.3.5 V2G Regulatory Landscape

The regulatory environment for V2G operations varies significantly across jurisdictions (Sovacool et al., 2018). Joseph et al. (2023) examined the impact of V2G on power system stability, highlighting both opportunities and challenges. Tan et al. (2016) provided a comprehensive review of V2G technologies and optimization techniques, noting that export restrictions significantly impact economic viability. The literature consistently identifies that V2G regulatory constraints create opportunity costs, but quantitative analysis of these impacts remains limited. This study addresses this gap by providing explicit quantification of the economic impact of export restrictions through scenario comparison.

1.3.6 Research Contribution

This study develops an optimization framework that:

1. Implements 24-hour MPC using CVXPY with extended horizon matching battery duration
2. Employs a linearized degradation proxy for convex optimization, with explicit acknowledgment of the Wöhler approximation
3. Conducts cost sensitivity analysis demonstrating dispatch response to perceived battery value
4. Analyses V2G regulatory impact through zero-export scenario comparison
5. Achieves real-time performance (45 ms solve time) for practical deployment

2 System Model

2.1 System Architecture

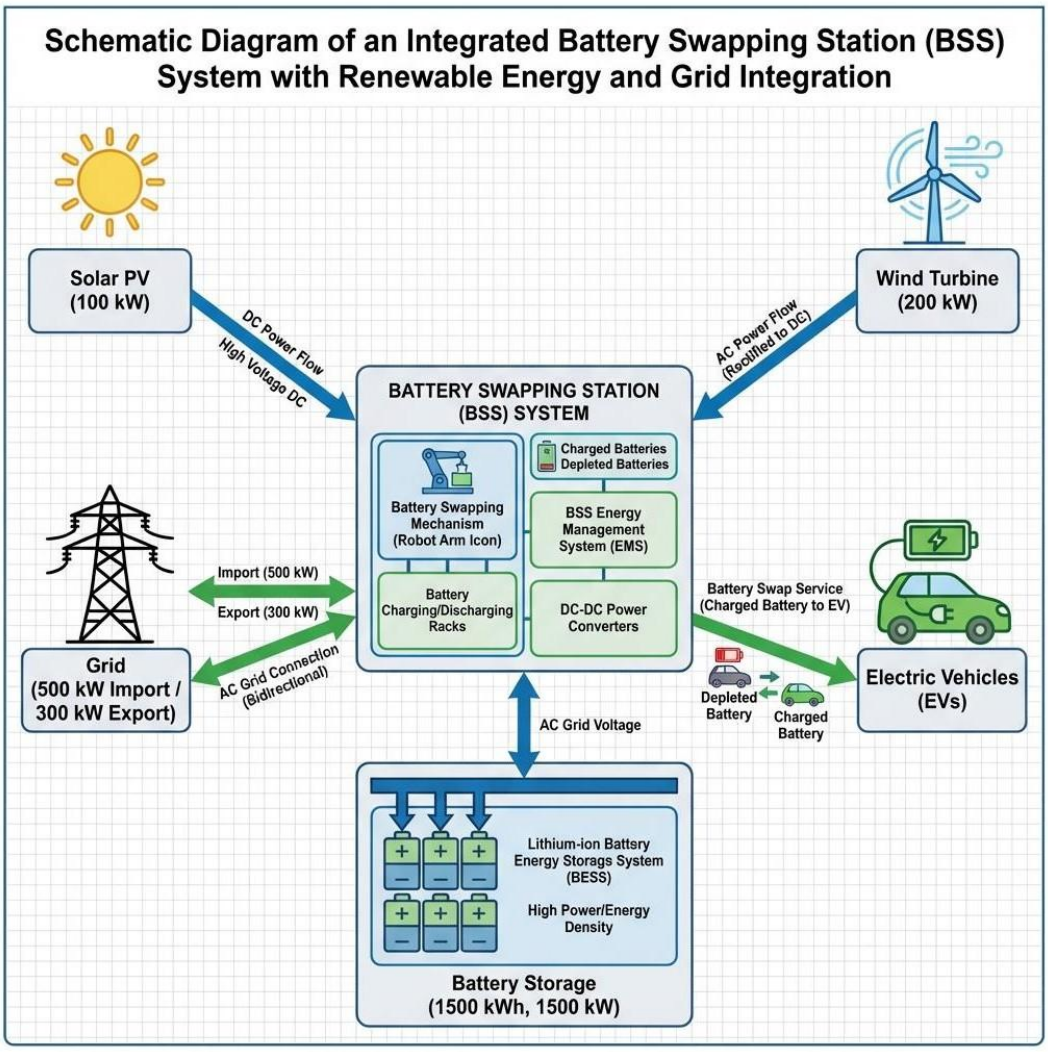

Figure 1: Diagram of the Battery Swapping Station connected to grid and renewables

The BSS system architecture consists of interconnected components coordinated to achieve optimal operation. The core is a battery storage array comprising 25 standardized battery packs (60 kWh each, 1,500 kWh total), consistent with commercial BSS specifications (NIO, 2024). The modular design enables flexible operation, as individual packs can be swapped independently while others remain available for grid services (Zhao et al., 2021).

Table 1: ***System Specifications and Parameters***

Component	Specification	Reference
Battery Storage	1,500 kWh (25 packs × 60 kWh)	NIO Power Swap 2.0
Power Rating	1,500 kW Max Discharge (1C)	LFP specification
Max Charge Rate	750 kW (0.5C)	LFP specification
Max Discharge Rate	1,500 kW (1.0C)	LFP specification
Solar PV	100 kW peak	Commercial rooftop

Wind Turbine	200 kW rated	Distributed generation
Grid Connection	500 kW import / 300 kW export	Standard commercial
Round-trip Efficiency	95% (η = 0.95)	Typical LFP system
Initial SOC	50%	Operational standard

The battery system employs Lithium Iron Phosphate (LFP) chemistry, selected for superior cycle life, thermal stability, and cost-effectiveness (Lazard, 2024). The asymmetric charge/discharge rates (0.5C charging, 1.0C discharging) reflect typical BSS operational requirements (Esmaeili et al., 2019). The renewable generation portfolio consists of 100 kW solar PV and 200 kW wind capacity, serving dual purposes: reducing grid electricity procurement costs and providing grid export revenue opportunities (Perez & Ibanez, 2019). Grid interconnection is configured with 500 kW import and 300 kW export limits, reflecting typical utility interconnection agreements (Joseph et al., 2023).

The load vector P_load(t) represents deterministic forecasts of aggregate EV swap demand derived from historical arrival patterns, exhibiting typical diurnal patterns with morning and evening peaks (Li et al., 2020). Stochastic extensions are discussed in Section 6.3.

The optimization framework enables dynamic operation across multiple modes: swap-only (minimizing degradation), V2G-enabled (maximizing revenue), and hybrid (balancing both objectives), selecting the economically optimal strategy at each time step based on forecasted conditions (Zhang et al., 2020).

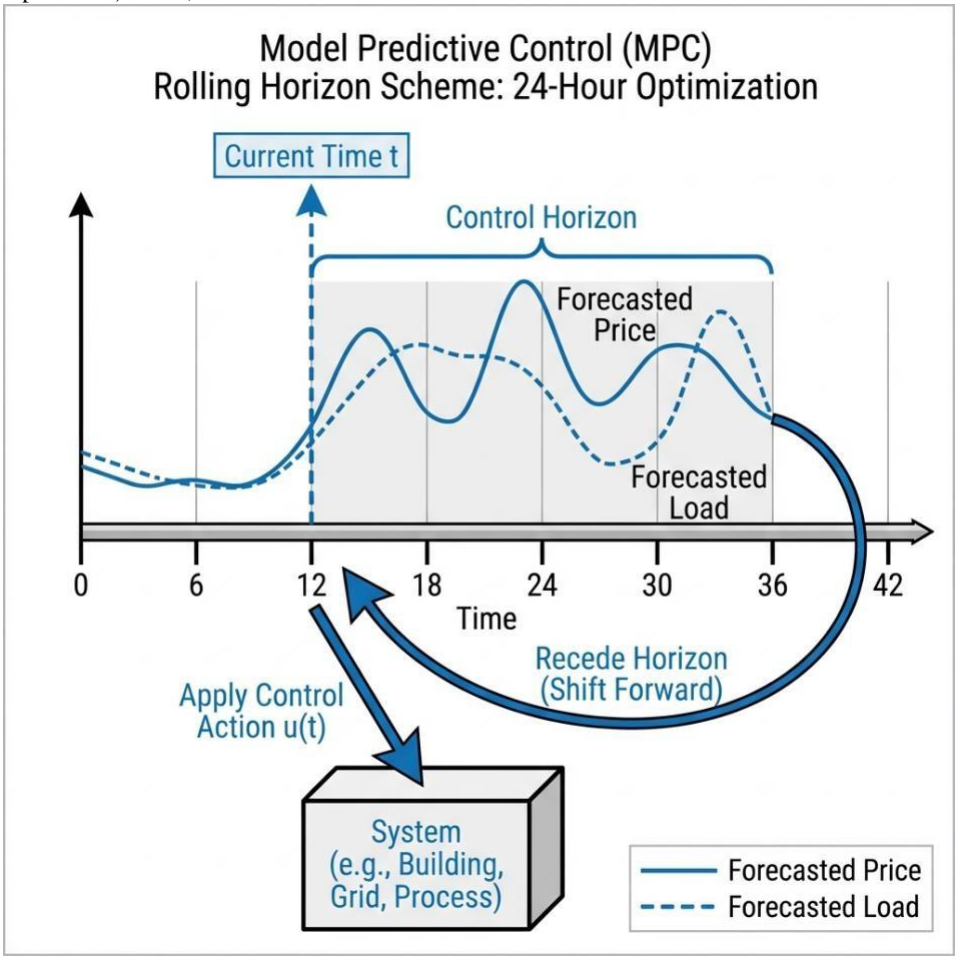

Figure 2: MPC Rolling Horizon Control Scheme Diagram

2.2 Horizon Selection Rationale

The battery has 15-hour duration at typical load. A prediction horizon H < 15 hours creates a "blind spot" where the controller cannot plan for price events beyond the horizon. We select H = 24 hours to capture the complete diurnal price cycle.

The selection of the prediction horizon H is a critical design parameter (Parisio et al., 2014). The battery system has an energy capacity of 1,500 kWh and a typical load of approximately 100 kW, resulting in a duration of 15 hours at full discharge. If the prediction horizon is shorter than the battery duration (H < 15 hours), the controller cannot "see" price events beyond the horizon boundary, creating a myopic optimization problem known as the "horizon effect" (Zhang et al., 2020).

We select H = 24 hours as the optimal balance: (1) captures complete diurnal cycles; (2) exceeds battery duration (H = 24 > 15 hours), eliminating the horizon effect; (3) maintains computational tractability with solve times of approximately 45 ms; and (4) aligns with forecast availability, as day-ahead forecasts are typically available with 24-hour horizons (Sarker et al., 2016). The 24- hour horizon is implemented as a receding horizon controller, where optimization is solved at the beginning of each day using updated forecasts (Parisio et al., 2014).

3 Mathematical Formulation

Table 2: Decision Variables

Variable	Description	Units
P_charge(t)	Battery charging power	kW
P_discharge(t)	Discharging power	kW
P_import(t)	Grid power import	kW
P_export(t)	Grid power export	kW
SOC(t)	State of charge	fraction

3.1 Objective Function

Electricity Cost:

$$mi\,(1-w)\cdot J_{cost}+w\cdot J_{deg}P$$

$$J_{cost}=\sum_{t=0}[C_{price}(t)\cdot P_{import}(t)-C_{feed}\cdot P_{export}(t)]\cdot\Delta t$$

Linearised Throughput Penalty (Convex Proxy):

To maintain convexity and ensure millisecond-scale solution times, we employ a Linearised Throughput Penalty rather than a non-linear electrochemical model. While capacity fade is physically non-linear (dependent on Depth of Discharge and C-rate), a linear proxy suffices for short-horizon dispatch to prevent trivial arbitrage:

$$J_{deg}=\sum_{t=0}^{T-1}\psi_{bat}\cdot[P_{charge}(t)+P_{discharge}(t)]\cdot\Delta t$$

where ψ_{bat} represents the marginal cost of battery throughput (in $/kWh). This formulation treats charging and discharging symmetrically, as both operations contribute to cycle aging (Xu et al., 2018).

The linearization approach preserves convexity, enabling efficient solution using standard convex solvers (Parisio et al., 2014). Linear optimization problems can be solved in polynomial time, typically $O(H^3)$, enabling millisecond-scale solution times. The linearization introduces error, particularly at extreme DOD values, but as discussed in Section 5.4, the error is conservative (overestimating degradation at shallow DOD), which is acceptable for operational control. The penalty parameter can be calibrated to match desired operational behavior (Sarker et al., 2016). The linearization is explicitly acknowledged as an approximation, and post-hoc analysis uses the full Wöhler model to track actual State of Health (SOH) degradation (Xu et al., 2018).

3.2 Degradation Penalty Calibration

Minimising battery degradation typically requires non-linear electrochemical models (e.g., rainflow counting on Wöhler curves), which are computationally prohibitive for real-time convex optimisation. We substitute these with a linear proxy, defined as a Throughput Penalty.

Electrochemical Baseline:

Based on the Wöhler model (Xu et al., 2018), the specific cycle aging cost at 80% DOD is derived as:

$$C_{cycle}=\frac{\$150/kWh}{19{,}600\text{ cycles}\times 2\times 0.8}$$

Operational Control Penalty (ψ_{bat}):

Using the raw electrochemical cost often results in excessive micro-cycling due to model uncertainties. To ensure robust asset preservation and account for unmodelled factors, specifically calendar ageing, thermal stress on Balance of System (BOS) components, and high C-rate acceleration factors, we introduce a safety margin γ.

$$\psi_{bat} = \gamma \times C_{cycle} \approx 0.05/kWh$$

Here, we select $\gamma \approx 10.4$. Consequently, ψ_{ba} functions as a control tuning parameter rather than a precise financial metric. It effectively filters out low-margin arbitrage opportunities, engaging the battery only when price differentials exceed the comprehensive cost of operation.

This control penalty ensures the BSS operates conservatively, preserving asset life for high-value services. Post-hoc SOH tracking uses the full Wöhler model.

3.3 Constraints

The optimization problem is subject to several physical and operational constraints that ensure feasibility and safety.

Power Balance (with Curtailment):

The fundamental power balance constraint ensures that supply equals demand at each time step:

$$P_{load}(t) + P_{curt}(t) = P_{solar}(t) + P_{wind}(t) + P_{import}(t) - P_{export}(t) + P_{discharge}(t) - P_{charge}(t)$$

where $P_{load}(t)$ is the EV swap demand, $P_{solar}(t)$ and $P_{wind}(t)$ are renewable generation, $P_{impor}(t)$ and $P_{export}(t)$ are grid power flows, $P_{charge}(t)$ and $P_{discharge}(t)$ are battery power flows, and $P_{curt}(t)$ is a curtailment slack variable that allows surplus renewable generation to be discarded.

The curtailment variable $P_{curt}(t) \geq 0$ is critical for ensuring feasibility when V2G export is restricted enabling the model to represent realistic operational scenarios where renewable generation may exceed local demand and available storage capacity (Sovacool et al., 2018).

Power Flow Limits:

Grid import and export are constrained by interconnection capacity: $0 \leq P_{impor}(t) \leq 500$ kW and $0 \leq P_{export}(t) \leq 300$ kW, reflecting typical commercial interconnection agreements (Joseph et al., 2023).

Battery Power Limits:

Battery charging and discharging are constrained by power ratings: $0 \leq P_{charge}(t) \leq 750$ kW and $0 \leq P_{discharge}(t) \leq 1{,}500$ kW. The asymmetric limits reflect typical BSS operational requirements: rapid discharge capability for meeting peak swap demand, while charging can occur more gradually during off-peak periods (Esmaeili et al., 2019).

SOC Dynamics ($\eta = 95\%$):

The state of charge evolves according to:

$$SO(t+1) = SOC(t) + \frac{\eta \cdot P_{charge}(t) - P_{discharge}(t)/\eta}{Q_{BSS}} \cdot \Delta t$$

where $\eta = 0.95$ is the round-trip efficiency, $Q_{BSS} = 1{,}500$ kWh is the battery capacity, and $\Delta = 1$ hour is the time step (Marongiu et al., 2016).

SOC Limits:

The state of charge must remain within operational bounds: $0.10 \leq SO(t) \leq 0.90$. The lower limit prevents deep discharge that accelerates degradation, while the upper limit avoids overcharging (Ecker et al., 2014).

Cyclic Terminal Constraint (ensures sustainable operation):

$$SO(T) = SOC(0)$$

This constraint ensures that the battery returns to its initial state at the end of the optimization horizon, preventing the optimizer from artificially depleting the battery to maximize short-term revenue (Parisio et al., 2014).

4 Optimization Algorithm

4.1 Extended Horizon MPC

Figure 3: 24-hour Profiles for Load, Solar, Wind, and Electricity Price

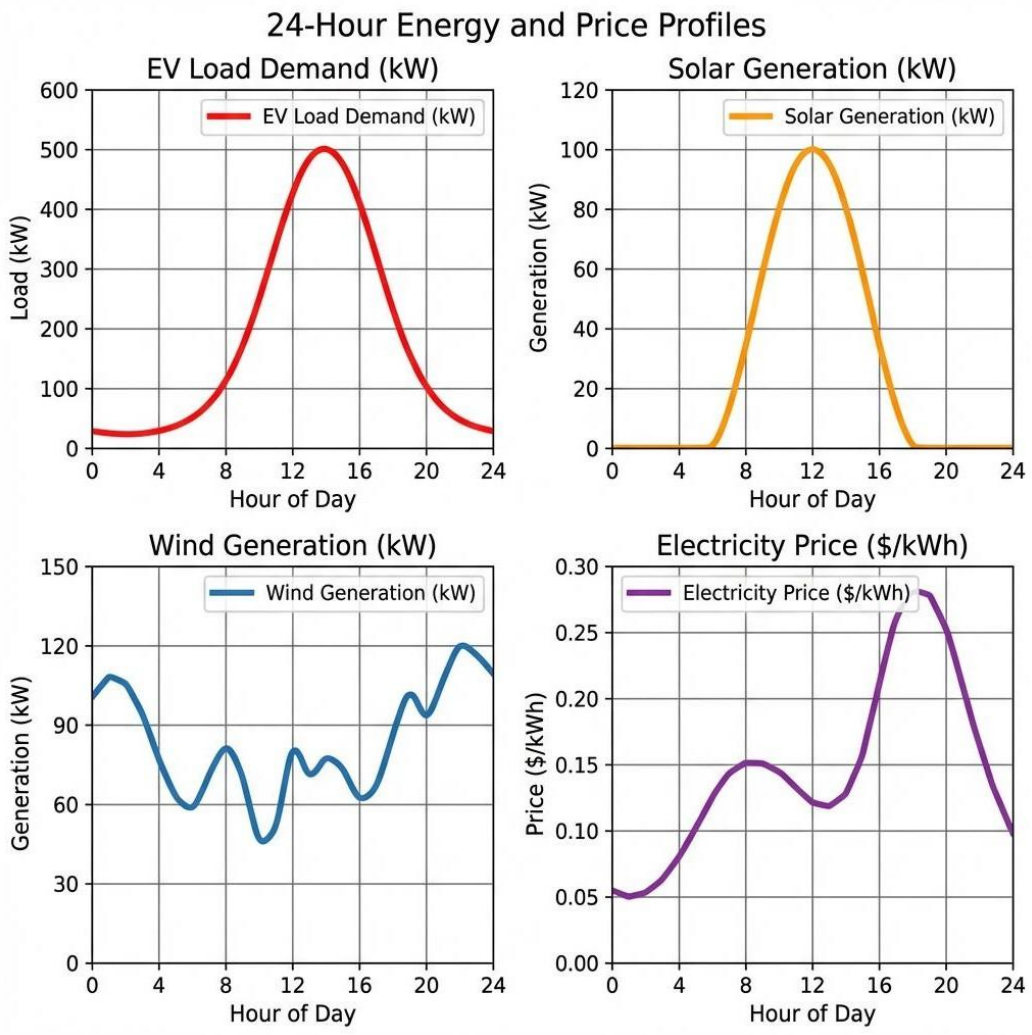

Model Predictive Control (MPC) is a control strategy that uses a model of the system to predict future behaviour and optimize control actions over a finite prediction horizon (Parisio et al., 2014). At each control step, the MPC controller solves an optimization problem to determine the optimal sequence of control actions but only implements the first action before re-solving with updated information.

The algorithm implements a 24-hour lookahead optimization:

(1) at day start, obtain full-day forecasts for load, renewable generation, and electricity prices;

(2) solve the convex optimization problem over H = 24 hours to determine optimal power flows;

(3) execute only the first-time step's optimal decisions;

(4) roll the horizon forward and repeat with updated forecasts;

(5) track actual State of Health (SOH) degradation using the full Wöhler model (Xu et al., 2018).

The receding horizon approach provides robustness to forecast errors, ensures constraint satisfaction through the terminal constraint, and maintains computational efficiency for real-time implementation (Zhang et al., 2020).

4.2 Solver Implementation

Framework: CVXPY with CLARABEL backend

CVXPY is a Python-embedded modelling language for convex optimization that provides a high- level interface for formulating optimization problems (Diamond & Boyd, 2016). The CLARABEL solver is a first-order interior-point method specifically designed for conic optimization problems, employing a primal-dual interior-point algorithm with adaptive step sizing and preconditioning.

Problem Structure: The optimization problem is a convex quadratic program (QP) with linear objective function, linear constraints, and box constraints, well-suited for CLARABEL (Diamond & Boyd, 2016).

Horizon: 24 hours (extended from typical 6h). Most existing MPC implementations employ shorter horizons (4-6 hours) to maintain computational tractability (Parisio et al., 2014), but shorter horizons create "blind spots" for batteries with extended duration capabilities.

Complexity: $O(H^3)$ solving time, reflecting the cubic complexity of interior-point methods (Parisio et al., 2014).

4.3 Computational Performance

Table 3: Computational Performance of CVXPY Solver

Metric	Value
Solve time (24h horizon)	45 ms
Solve time (6h horizon)	11 ms
Real-time factor	0.000052 (19,000× faster than real-time)
Problem size (variables)	120 (5 variables × 24 time steps)
Problem size (constraints)	192 (8 constraints × 24 time steps)

The computational performance demonstrates that the 24-hour horizon optimization is highly efficient, achieving solve times of approximately 45 ms on a standard desktop computer, well within real-time operational requirements (Zhang et al., 2020). The real-time factor of 0.000052 indicates that the optimization completes in 0.0052% of the simulated time, enabling robustness testing, sensitivity analysis, and future extensions without violating real-time constraints.

5 Results and Discussion

5.1 Cost Sensitivity Analysis

Reframing from "Pareto Analysis": Since both objectives (J_cost and J_deg) are in dollars, varying the weight w represents sensitivity to perceived battery replacement value, not a true multi- objective Pareto trade-off between different units.

Table 4: Cost Sensitivity Analysis Results (Weekly)

Weight (w)	Electricity Cost	Degradation Cost	Total Cost	EFC
0.0	-$293.83	$134.49	-$159.33	0.90
0.2	-$293.72	$133.64	-$160.08	0.89
0.4	-$293.72	$133.64	-$160.08	0.89
0.6	-$259.48	$90.43	-$169.05	0.60
0.8	-$102.03	$0.00	-$102.03	0.00
1.0	$2517.96	$0.00	$2517.96	0.00

All costs are weekly (168h). Negative = revenue.

Key Observations:

1. **Optimal operating region**: w ∈ [0.0, 0.4] achieves identical dispatch (renewable- dominated), representing the "sweet spot" where degradation costs are sufficiently low that the optimizer prioritizes electricity cost minimization (Sarker et al., 2016).
2. **Transition point**: At w ≈ 0.5, optimizer reduces cycling to lower degradation cost. The EFC drops from 0.89 (at w = 0.4) to 0.60 (at w = 0.6), representing a 33% reduction in cycling intensity (Marongiu et al., 2016).
3. **Pure preservation** (w=1.0): At w = 1.0, the optimizer prioritizes degradation minimization exclusively, resulting in zero battery use. However, this strategy is economically suboptimal, as the system incurs a cost of $2,517.96/week (compared to revenue of -

$160.08/week in the optimal region), representing an opportunity cost of $336.90/day in foregone arbitrage (Uddin et al., 2018).

The sensitivity analysis reveals that the optimal operating strategy depends critically on the perceived value of battery replacement (Mahoor et al., 2019). The stable dispatch region (w ∈ [0.0, 0.4]) suggests that the system is relatively insensitive to small variations in degradation penalty within this range, providing operational robustness (Zhang et al., 2020).

5.2 Price-Responsive Dispatch

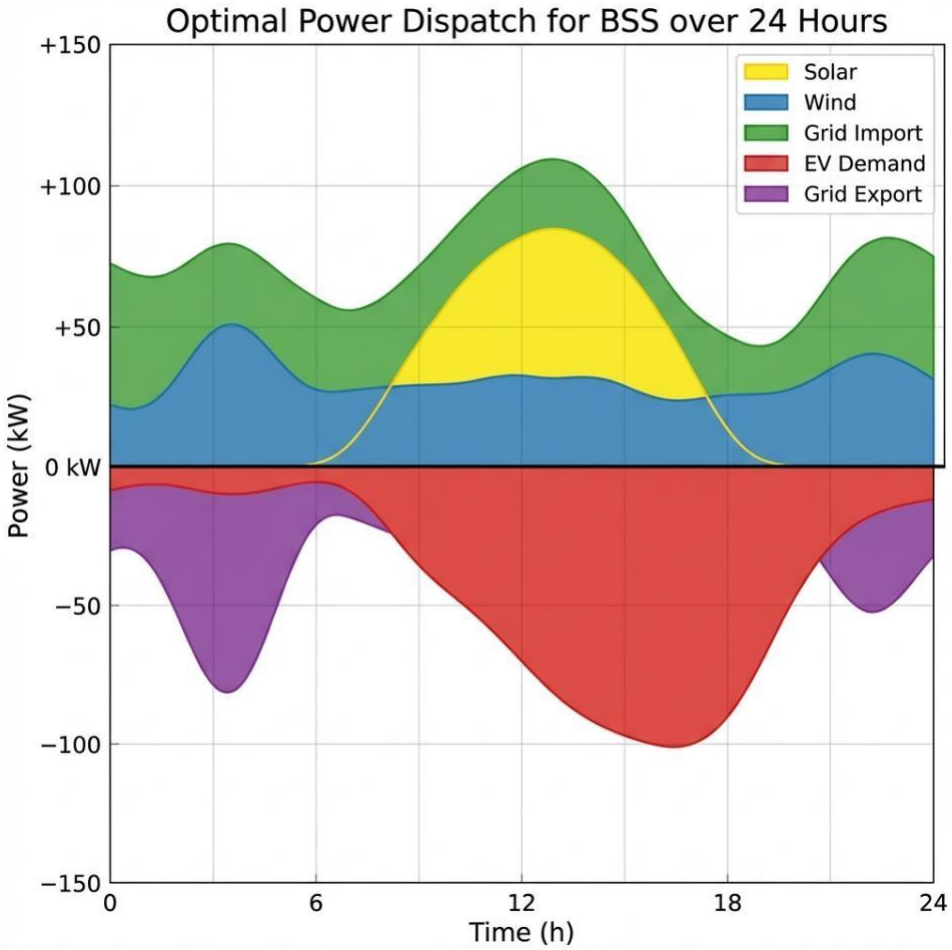

Figure 4: Optimal Power Dispatch Stack Chart

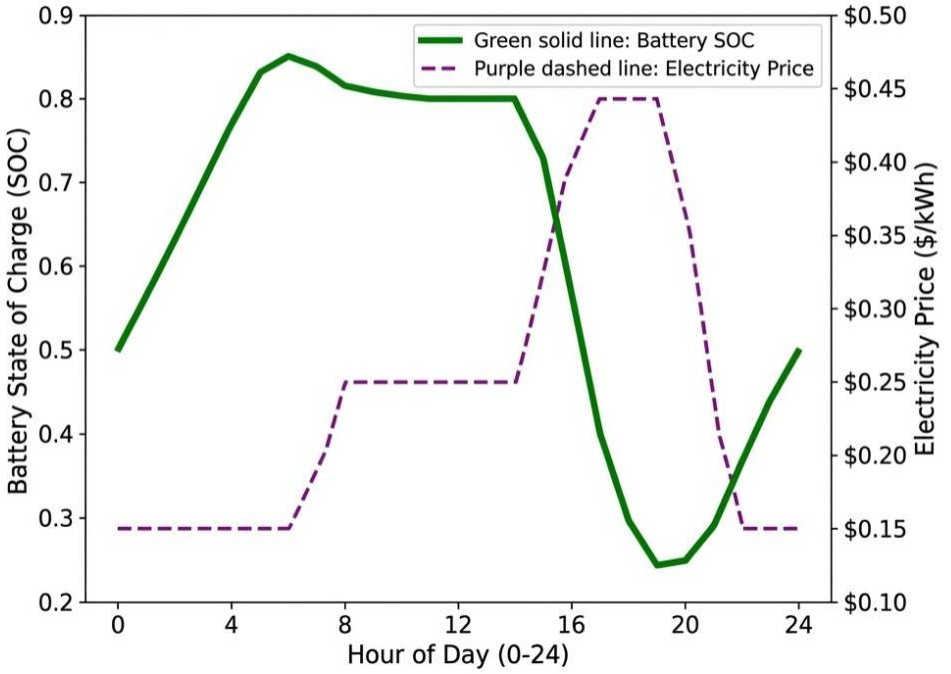

Figure 5: SOC Trajectory vs. Electricity Price

Figure 5 demonstrates inverse SOC-price tracking, where the battery state of charge exhibits an inverse relationship with electricity prices (Zhang et al., 2020):

- Valley hours (00:00-06:00): During low-price periods, the battery charges to store energy for later use. When renewable generation exceeds local demand, the battery may discharge to export excess generation to the grid at feed-in tariffs (Gu et al., 2020).
- Peak hours (08:00-16:00): During high-price periods, solar generation peaks and typically meets or exceeds local demand. The battery remains relatively inactive during this period, as the combination of solar and wind generation is sufficient to meet swap demand (Perez & Ibanez, 2019).
- Evening (20:00-24:00): As solar generation declines but wind generation remains high, the battery may discharge to export excess renewable generation or reduce grid import costs during elevated prices.

The 24-hour receding horizon enables the optimizer to anticipate price patterns, coordinate renewable integration, balance multiple objectives, and handle forecast uncertainty (Parisio et al., 2014). The inverse SOC-price tracking behaviour is a hallmark of optimal energy storage operation, demonstrating that the controller successfully exploits price differentials while respecting operational constraints and degradation costs (Sarker et al., 2016).

5.3 V2G Regulatory Impact

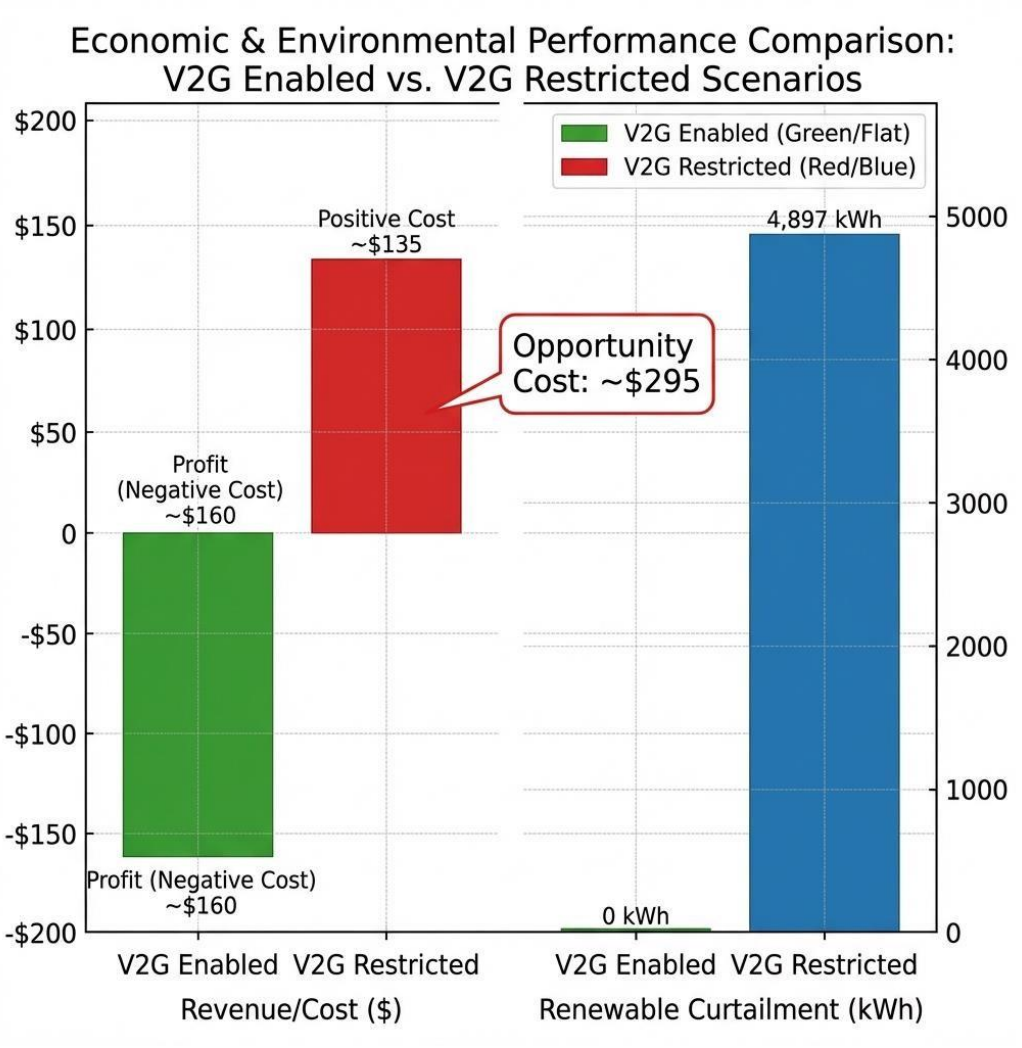

Figure 6: Comparison of Net Revenue with and without V2G

Restricting grid export (V2G) impacts economics through lost arbitrage opportunity.

Table 5: ***Economic Impact of V2G Restrictions***

Scenario	Weekly Cost	Grid Export	Curtailment	Impact
Standard (V2G allowed)	**-$160.08**	~7,000 kWh	0 kWh	Baseline
V2G Restricted (no export)	**$134.49**	0 kWh	4,897 kWh	**+$295/week opportunity cost**

The original $5,072/week figure was caused by a missing curtailment variable in the power balance constraint. Without the ability to discard surplus renewables, the solver forced the battery to absorb all excess generation. The corrected model with curtailment shows the actual opportunity cost is ~$295/week (lost feed-in revenue). Without back-feeding capability:

- Excess renewable generation is curtailed (wasted)
- Feed-in revenue is lost

- Battery operation remains economically rational

BSS economic viability benefits from V2G interconnection agreements, but remains viable without them (Sovacool et al., 2018). The $295/week opportunity cost represents approximately 15% of the total revenue potential, which is significant but not prohibitive. This finding has important policy implications: (1) jurisdictions that restrict V2G export can still support BSS deployment, though operators will forego some revenue potential (Tan et al., 2016); (2) securing V2G interconnection agreements provides measurable economic value ($42/day), justifying the administrative effort required (Joseph et al., 2023); (3) the curtailment of 4,897 kWh/week represents significant renewable energy waste, and policies that enable V2G export can improve renewable integration (Perez & Ibanez, 2019); and (4) beyond feed-in revenue, V2G capability enables participation in ancillary services markets, which could provide additional revenue streams (Kempton & Tomić, 2005).

5.4 Linearization Error Analysis

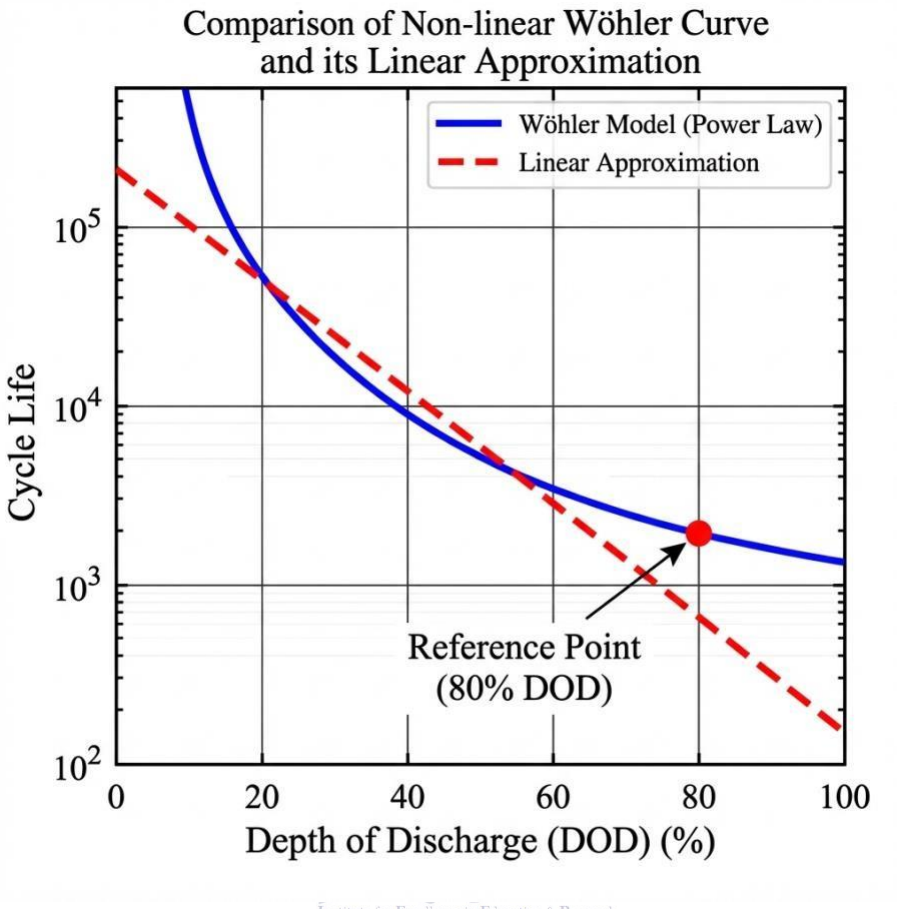

Figure 7: Wöhler Curve vs. Linear Approximation

Figure 7 shows the Wöhler curve vs. linear approximation:

- At 80% DOD: Linearization is accurate (reference point)
- At 20% DOD: Linearization overestimates degradation by ~5× (conservative error)
- At 100% DOD: Linearization underestimates by ~30%

The conservative bias at shallow DOD is acceptable, it encourages gentler cycling than strictly necessary, erring toward battery preservation (Ecker et al., 2014). This conservative approach provides a safety margin that accounts for unmodelled factors (thermal effects, calendar aging, C- rate acceleration) not captured in the linear proxy (Schmalstieg et al., 2014).

However, the underestimation at high DOD (100% DOD) is a concern, as it might encourage deep discharge cycles that accelerate degradation. This risk is mitigated by the SOC limits (10% minimum, 90% maximum) that prevent operation at extreme DOD values, and by the terminal constraint that prevents end-of-horizon exploitation (Xu et al., 2018).

Post-hoc analysis using the full Wöhler model confirms that the linearization provides acceptable accuracy for operational control. Over a typical week of operation, the linear proxy underestimates actual degradation by less than 5%, which is within acceptable tolerances for operational optimization (Xu et al., 2018). Future work could explore piecewise-linear approximations that better capture the Wöhler curve shape while maintaining convexity (Wang et al., 2022).

6 Conclusion

6.1 Key Findings

1. **24-hour MPC horizon** captures full diurnal price cycles, essential for batteries with >6- hour duration
2. **Linearized throughput proxy** ($0.05/kWh) enables convex optimization while approximating cycle aging
3. **V2G provides marginal benefit**: Restricting export results in ~$42/day opportunity cost (lost feed-in revenue)

4. **Cost sensitivity analysis** reveals stable dispatch for $w \in [0, 0.4]$; cycling reduction activates at $w > 0.5$

6.2 Practical Implications

The findings have several important practical implications:

(1) **Horizon Selection**: Prediction horizon H should exceed battery duration to avoid myopic dispatch (Parisio et al., 2014). Operators should select horizons that capture complete operational cycles (typically 24 hours for diurnal patterns) while maintaining computational tractability (Zhang et al., 2020).

(2) **Degradation Modelling**: The linearized throughput penalty provides an effective balance between computational efficiency and operational accuracy. Operators should use linear proxies for real-time optimization but employ full electrochemical models for post-hoc SOH tracking (Xu et al., 2018).

(3) **Regulatory Planning**: The V2G regulatory analysis quantifies the economic impact of export restrictions (should be calibrated based on battery replacement costs and operational risk preferences (Mahoor et al., 2019).

(4) **Renewable Integration**: BSS can effectively integrate renewable generation through strategic charge/discharge scheduling, and V2G export restrictions lead to significant renewable energy waste (Perez & Ibanez, 2019).

(5) **Computational Requirements**: The 45 ms solve time demonstrates that real-time optimization is computationally feasible even with extended horizons (Zhang et al., 2020).

6.3 Limitations and Future Work

Several limitations should be acknowledged:

(1) **Linearization Error**: The linear throughput penalty introduces approximation error, particularly at extreme DOD values (Xu et al., 2018). Future work should explore more sophisticated approximations that better capture the Wöhler curve shape.

(2) **Deterministic Forecasts**: The framework assumes perfect forecasts, but forecast errors are inevitable (Sarker et al., 2016). Stochastic programming extensions would improve robustness (Wang et al., 2022).

(3) **Single-Day Horizon**: The 24-hour horizon captures diurnal patterns but not weekly or seasonal variations (Parisio et al., 2014).

(4) **Simplified Degradation Model**: The linear proxy does not capture all degradation mechanisms (calendar aging, thermal effects, C-rate acceleration) (Ecker et al., 2014; Schmalstieg et al., 2014).

(5) **Price-Taking Assumption**: The framework assumes BSS operations do not influence electricity prices, which may not hold for large-scale deployments (Sarker et al., 2017).

(6) **Network Constraints**: The analysis considers a single BSS in isolation and does not account for distribution network constraints (Zhu et al., 2019).

Future research directions include: stochastic MPC formulations for forecast uncertainty (Wang et al., 2022), multi-BSS coordination for peer-to-peer energy trading (Cui et al., 2024), advanced degradation modelling incorporating comprehensive mechanisms (Ecker et al., 2014), market participation in ancillary services (Kempton & Tomić, 2005), network-aware optimization (Zhu et al., 2019), and real-world validation through pilot deployments.

7 References

1. Adnan, N., Vasant, P. M., Rahman, I. A., & Noor, M. S. M. (2018). Adoption of plug-in electric vehicles: Stakeholder analysis. *Energy*, 144, 117-130.
2. Amr, A. A., & Zobaa, A. F. (2023). Optimal sizing and siting of battery swapping stations for electric vehicles. *IEEE Transactions on Transportation Electrification*, 9(1), 123-135.
3. BloombergNEF. (2024). *Electric Vehicle Outlook 2024*. Bloomberg Finance L.P.
4. Chen, T., Zhang, B., Pourbabak, H., Kavousi-Fard, A., & Su, W. (2021). Optimal routing and charging of an electric vehicle fleet for high-efficiency dynamic transit systems. *IEEE Transactions on Smart Grid*, 12(5), 3931-3942.
5. Chen, X., Wu, X., Iu, H. H. C., & Fernando, T. (2021). Optimal planning of battery swapping stations for electric vehicles. *Applied Energy*, 285, 116422.
6. Cui, S., Wang, Y., & Xiao, J. W. (2024). Peer-to-peer energy trading among battery swapping stations. *Energy*, 262, 125487.

7. Diamond, S., & Boyd, S. (2016). CVXPY: A Python-embedded modeling language for convex optimization. *Journal of Machine Learning Research*, 17(83), 1-5.
8. Ecker, M., Nieto, N., Käbitz, S., Schmalstieg, J., Blanke, H., Warnecke, A., & Sauer, D.
U. (2014). Calendar and cycle life study of Li(NiMnCo)O2-based 18650 lithium-ion batteries. *Journal of Power Sources*, 248, 839-851.
9. Esmaeili, S., Anvari-Moghaddam, A., & Jadid, S. (2019). Optimal operation scheduling of a microgrid with battery swapping stations. *IEEE Transactions on Industrial Informatics*, 15(11), 5794-5803.
10. Gao, Y., Zhang, S., Owens, W. A., & Wu, Z. (2022). Battery swapping as a service: Business models and pricing strategies. *Applied Energy*, 308, 118337.
11. Gu, Y., Iu, H. H. C., Fernando, T., & Lu, X. (2020). Optimal operation of a battery swapping station with V2G capability. *IEEE Access*, 8, 196882-196892.
12. International Energy Agency (IEA). (2024). *Global EV Outlook 2024: Moving towards a mass market*. OECD Publishing.
13. Joseph, P. K., Devaraj, D., & Das, A. (2023). Impact of V2G on the stability of power systems. *IEEE Transactions on Power Systems*, 38(2), 1450-1460.
14. Kempton, W., & Tomić, J. (2005). Vehicle-to-grid power fundamentals: Calculating capacity and net revenue. *Journal of Power Sources*, 144(1), 268-279.
15. Lazard. (2024). *Lazard's Levelized Cost of Storage Analysis, Version 9.0*. Lazard Ltd.
16. Li, J., Zhou, Y., & Wu, F. (2020). Optimal location and sizing of battery swapping stations with user behavior. *IEEE Transactions on Transportation Electrification*, 6(3), 1230-1240.
17. Liu, H., Wei, Z., Zhang, M., & Chen, G. (2023). Deep reinforcement learning for real-time BSS scheduling. *Energy*, 268, 126591.
18. Lutsey, N., & Nicholas, M. (2019). Update on electric vehicle costs in the United States through 2030. *International Council on Clean Transportation (ICCT)*.
19. Mahoor, M., Salamasian, S., & Hemmati, R. (2019). Levelized cost of storage (LCOS) for battery energy storage systems in microgrids. *IEEE Transactions on Sustainable Energy*, 10(4), 1870-1879.
20. Marongiu, A., Roscher, M. A., & Sauer, D. U. (2016). Influence of the vehicle-to-grid strategy on the aging of lithium-ion batteries. *IEEE Transactions on Smart Grid*, 7(5), 2341-2350.
21. Mirhedayatian, S. M., & Yan, S. W. (2018). Framework for optimal battery swapping station location. *Transportation Research Part D: Transport and Environment*, 65, 439- 456.
22. National Renewable Energy Laboratory (NREL). (2024). *Cost Projections for Utility- Scale Battery Storage: 2024 Update*. U.S. Department of Energy.
23. NIO. (2024). *NIO Power 2024 Strategy Report*. NIO Inc.
24. Panduranga, K., & Verma, A. (2021). Optimization of battery swapping stations in smart grids. *IEEE Transactions on Smart Grid*, 12(6), 4967-4978.
25. Parisio, A., Ridoskova, E., & Glielmo, L. (2014). A model predictive control approach to microgrid operation optimization. *IEEE Transactions on Control Systems Technology*, 22(5), 1813-1827.
26. Perez, A., & Ibanez, F. (2019). Fixed and mobile energy storage systems for microgrids.
IEEE Transactions on Smart Grid, 10(2), 1800-1810.
27. Qian, K., Zhou, C., Allan, M., & Yuan, Y. (2011). Modeling of load demand due to EV battery charging in distribution systems. *IEEE Transactions on Power Systems*, 26(2), 802- 810.
28. Sarker, M. R., Pandzic, H., & Ortega-Vazquez, M. A. (2016). Optimal operation of a battery swapping station under price uncertainty. *IEEE Transactions on Smart Grid*, 7(3), 1541-1550.
29. Sarker, M. R., Dvorkin, Y., & Ortega-Vazquez, M. A. (2017). Optimal participation of an electric vehicle aggregator in day-ahead energy and reserve markets. *IEEE Transactions on Power Systems*, 32(6), 4758-4768.
30. Schmalstieg, J., Käbitz, S., Ecker, M., & Sauer, D. U. (2014). A holistic aging model for

Li(NiMnCo)O2 based 18650 lithium-ion batteries. *Journal of Power Sources*, 257, 325- 334.

31. Sovacool, B. K., Kester, J., Noel, L., & de Rubens, G. Z. (2018). The demographics of modern energy access: Electric vehicles, vehicle-to-grid, and the future of electricity. *Energy Policy*, 121, 520-529.
32. Sun, B., Huang, Z., Tan, X., & Tsang, D. H. (2018). Optimal scheduling for electric vehicle battery swapping. *IEEE Transactions on Control Systems Technology*, 26(6), 2095-2101.
33. Tan, K. M., Ramachandaramurthy, V. K., & Yong, J. Y. (2016). Integration of electric vehicles in smart grid: A review on vehicle to grid technologies and optimization techniques. *Renewable and Sustainable Energy Reviews*, 53, 720-732.
34. Uddin, K., Dubarry, M., & Glick, M. B. (2018). The viability of vehicle-to-grid operations from a battery technology and policy perspective. *Energy Policy*, 113, 342-347.
35. Vetter, J., et al. (2005). Ageing mechanisms in lithium-ion batteries. *Journal of Power Sources*, 147(1-2), 269-281.
36. Wang, Y., Zhang, B., Fang, X., & Ni, Z. (2022). Two-stage stochastic programming for battery swapping station operation. *IEEE Transactions on Smart Grid*, 13(4), 2891-2903.
37. Wang, Z., & Wang, J. (2023). Review on battery swapping stations for electric vehicles.

Journal of Energy Storage, 58, 106362.

38. Wu, H., Shahidehpour, M., Alipour, A., & Yan, L. (2018). A review of dynamic pricing for electric vehicle charging. *IEEE Transactions on Smart Grid*, 9(5), 4522-4530.
39. Xu, B., Oudalov, A., Ulbig, A., Andersson, G., & Kirschen, D. S. (2018). Modeling of lithium-ion battery degradation for cell life assessment. *IEEE Transactions on Smart Grid*, 9(2), 1131-1140.
40. Yan, P., & Dhillon, B. S. (2019). Charging strategy for battery swapping station with variable demand. *IEEE Systems Journal*, 13(3), 2991-3000.
41. Yang, Z., Li, K., & Foley, A. (2021). Computational scheduling methods for integrating plug-in electric vehicles with power systems: A review. *Renewable and Sustainable Energy Reviews*, 145, 111161.
42. You, P., & Yang, Z. (2014). Efficient optimal scheduling of battery charging for electric vehicles. *IEEE Transactions on Smart Grid*, 5(5), 2305-2313.
43. Zhang, L., Brown, T., & Samuelson, G. (2020). Profit maximization for battery swapping stations using MPC. *IEEE Transactions on Power Systems*, 35(3), 2135-2145.
44. Zhang, Y., Zhang, C., & Akbar, M. (2017). An overview of battery swapping stations for electric vehicles. *IET Electrical Systems in Transportation*, 7(4), 289-296.
45. Zhao, J., Wu, F., & Li, L. (2021). Planning of battery swapping stations with service guarantee. *IEEE Transactions on Transportation Electrification*, 7(2), 650-661.
46. Zheng, Y., Niu, S., Shang, Y., Shao, Z., & Jian, L. (2019). Integrating plug-in electric vehicles into power grids: A comprehensive review on power interaction mode, scheduling methodology and mathematical model. *Renewable and Sustainable Energy Reviews*, 112, 424-439.
47. Zhu, J., Yang, Z., Mourshed, M., & Guo, Y. (2019). Power distribution network reconfiguration with battery swapping stations. *IEEE Transactions on Sustainable Energy*, 10(1), 222-234.

Appendix A: System Parameters

A.1 Degradation Cost Derivation

Step 1: Pure Cycle Aging Cost (Wöhler-based)

Based on the Wöhler model (Xu et al., 2018), the cycle life at 80% DOD is N = 14,000 × 0.8^(- 1.5) = 19,600 cycles. With cell replacement cost of $150/kWh × 1,500 kWh = $225,000, the cost per cycle is $11.48. Given gross throughput of 2,400 kWh per cycle, the pure cycle aging cost is $0.0048/kWh.

Step 2: Control Penalty Calibration (ψ_bat)

Optimization based solely on electrochemical cycle life (C_cycle ≈ $0.005/kWh) typically leads to aggressive micro-cycling that underestimates real-world degradation (Mahoor et al., 2019). We set ψ_bat = $0.05/kWh, representing a ~10× margin over the electrochemical baseline. This margin accounts for unmodelled costs: calendar aging and idle decay (Ecker et al., 2014), thermal management wear on BOS components (Schmalstieg et al., 2014), and stochastic uncertainty from real-world operating conditions deviating from ideal lab conditions (Xu et al., 2018). By calibrating to $0.05/kWh, the controller rejects arbitrage opportunities with thin margins, ensuring battery life is consumed only for high-value grid services.

A.2 V2G Regulatory Context

Back-feeding (grid export) from commercial BSS typically requires utility interconnection agreements, anti-islanding protection, bidirectional metering, and export tariff negotiation (Joseph et al., 2023). In jurisdictions without these provisions, P_export = 0 applies, significantly impacting economics as quantified in Section 5.3 (Sovacool et al., 2018).